A

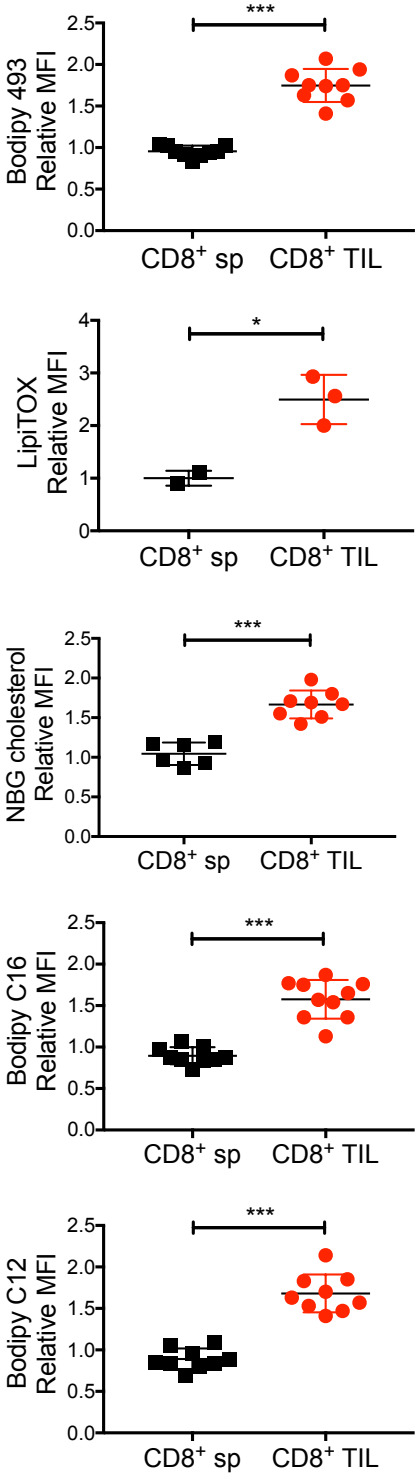

B

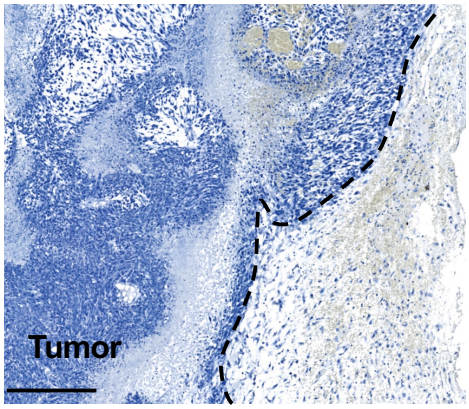

Figure S1, related to Figure 1

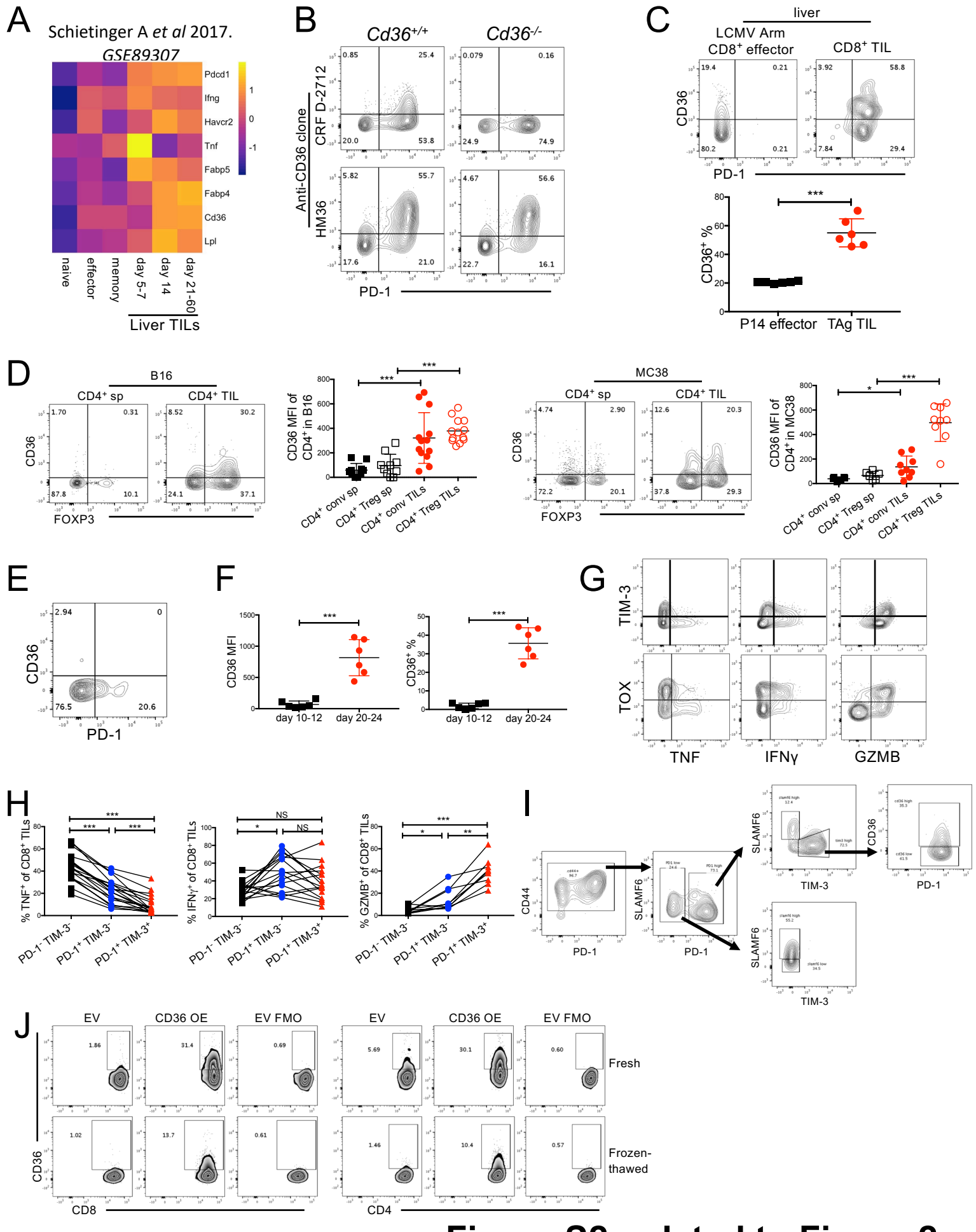

Figure S2, related to Figure 2

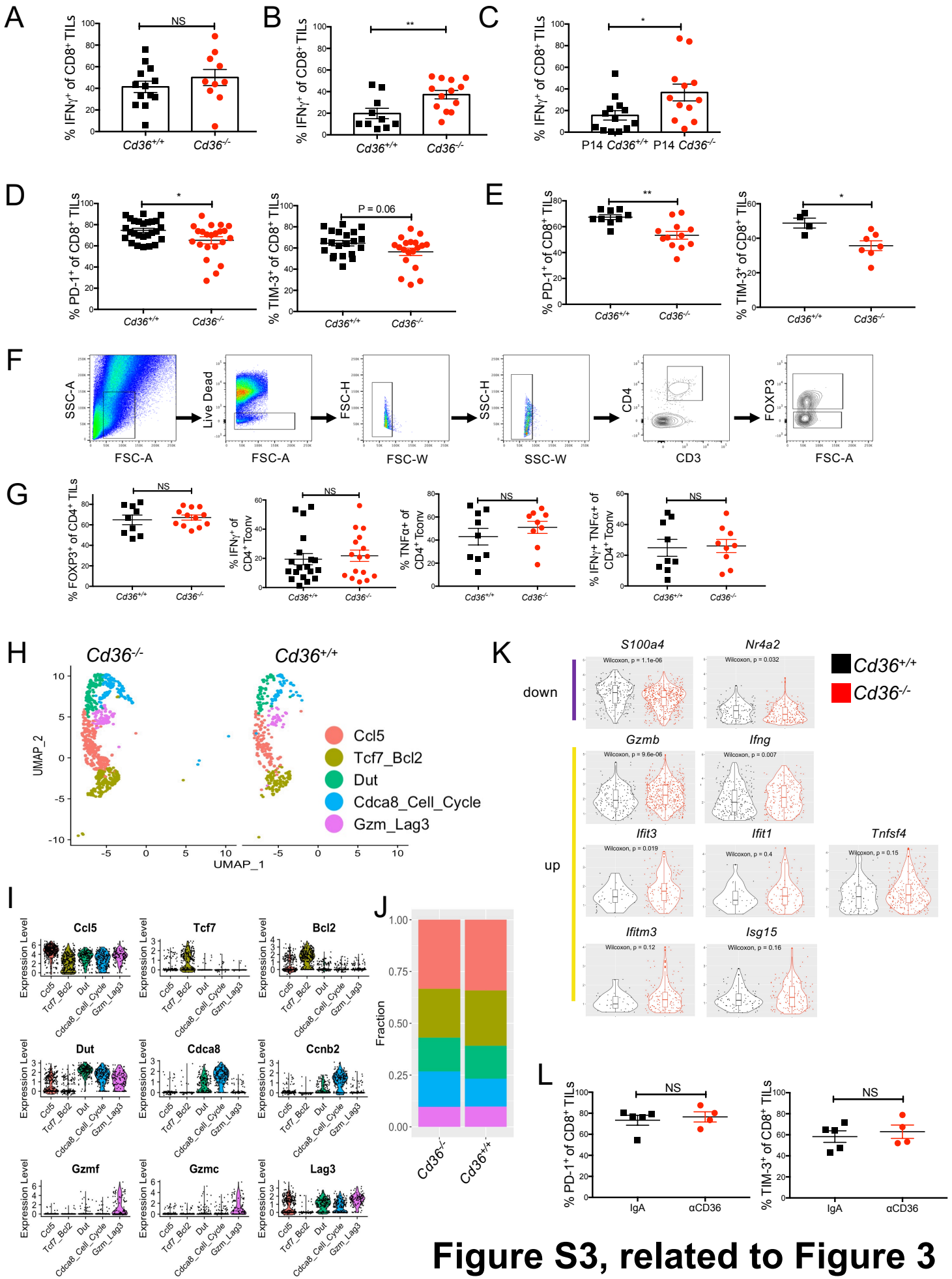

Figure S3, related to Figure 3

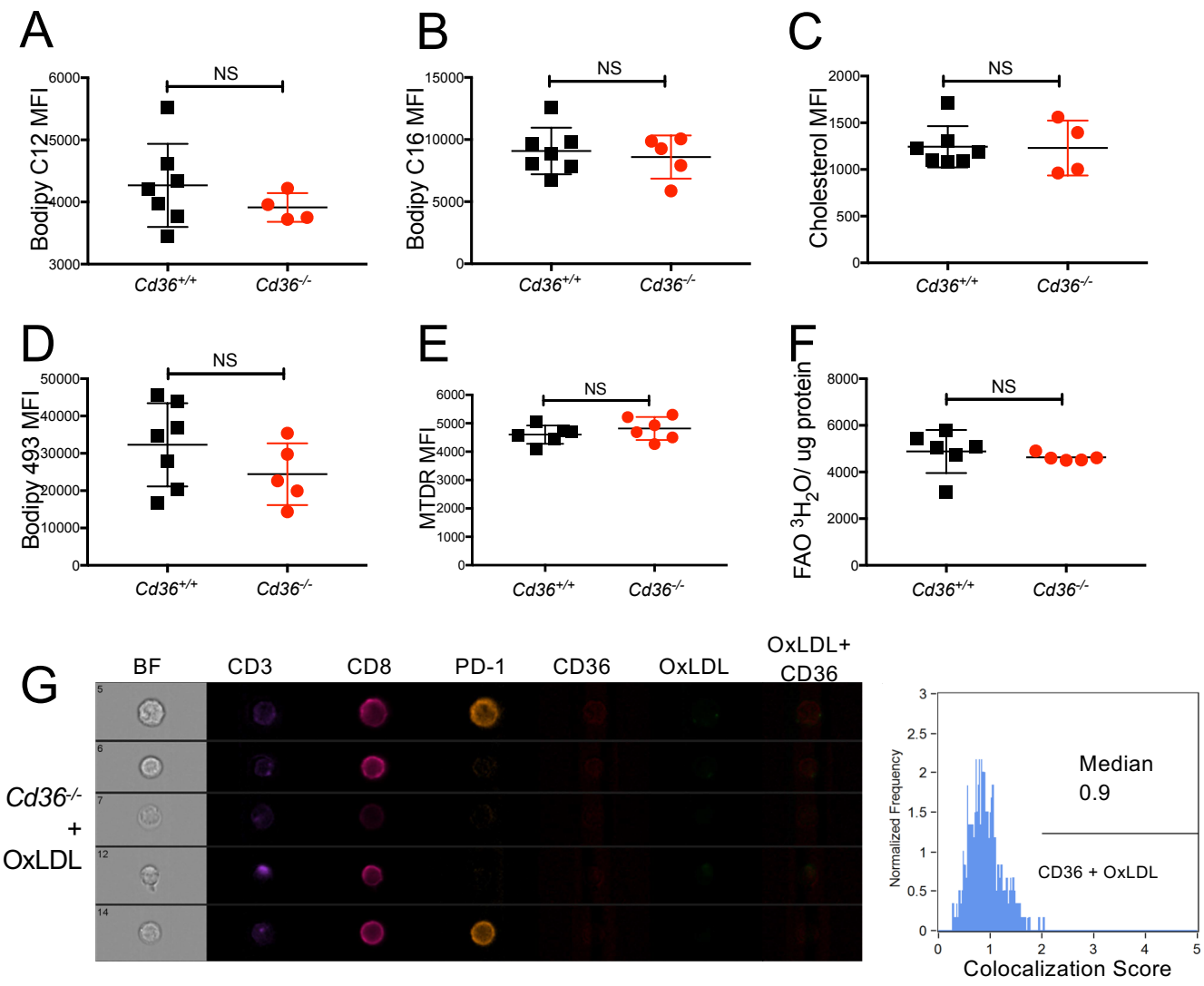

Figure S4, related to Figure 4

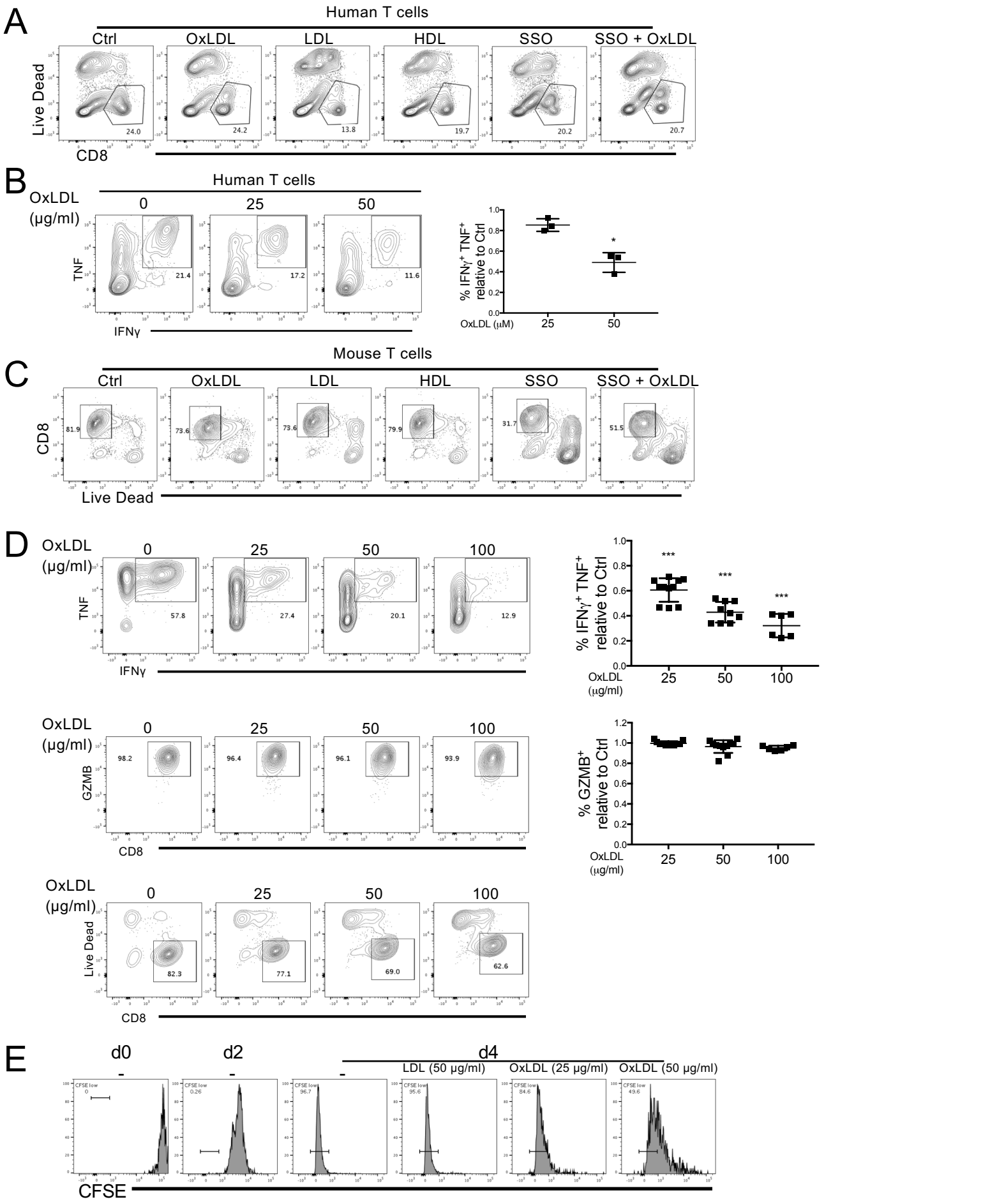

Figure S5, related to Figure 5

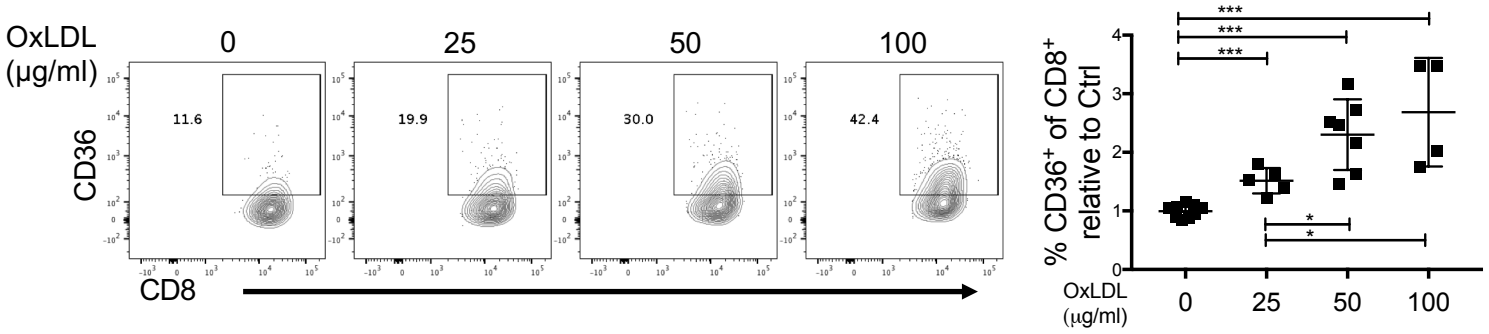

Figure S6, related to Figure 6

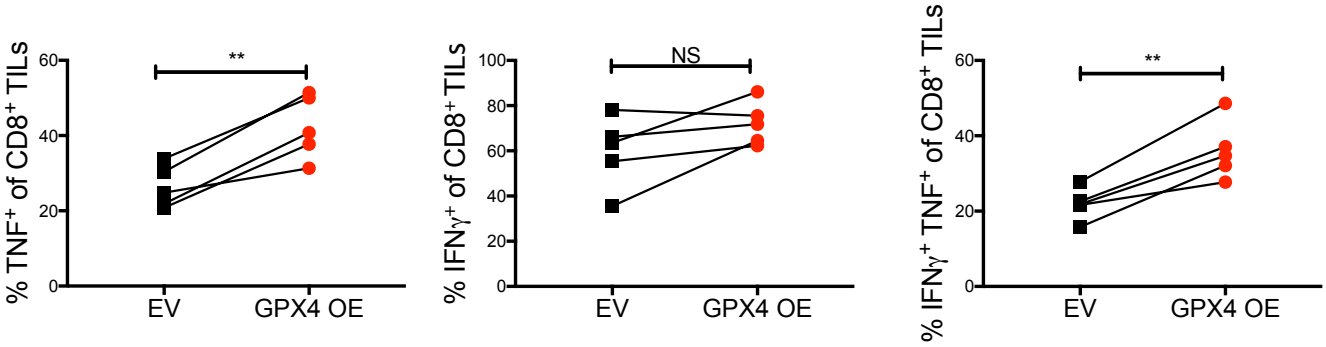

Figure S7, related to Figure 7

Supplemental Figure Legends

Figure S1. Increased lipid uptake and storage in CD8$^+$ TILs in murine tumors

(A-B) C57BL/6J mice were implanted with MC38 (A) or B16 (B) tumor cells as indicated below and tumors or splenocytes were examined 21 days later.

(A) Neutral lipid content (Bodipy 493 or LipidTOX), uptake of cholesterol and fatty acids (NBD cholesterol, Bodipy C12, and Bodipy C16) was compared between CD8$^+$ T cells isolated from the spleen (CD8$^+$ sp) or tumors (CD8$^+$ TILs) by flow cytometry. Congenic Thy1.1 naïve splenocytes were spiked into each well to control for sample-to-sample variation and serve as an internal reference for normalizing Bodipy or NBD staining. Data shown are mean ± SEM and statistical analysis was performed by two-tailed unpaired Student's t-test, * $p < 0.05$, ***$p < 0.001$. All the results were pooled from 2-3 experiments with n=2-10.

(B) Negative staining of B16 tumors by anti-mouse IgM secondary antibody in the absence of IgM E06 primary. The nuclei were stained with hematoxylin. Scale bar, 250 μm.

Figure S2. CD36 is expressed on functionally exhausted CD8$^+$ TILs and regulatory CD4$^+$ TILs

(D-I) C57BL/6J mice were implanted with B16 or MC38 tumor cells as indicated below, and tumors or splenocytes were examined 21 days later unless specified.

(A) The transcript levels of indicated genes in naïve, effector, memory TCR_{TAG} CD8$^+$ T cells (specific for SV40 large T antigen epitope I (TAG)) from TAG-expressing *Listeria monocytogenes*-infected spleens or tumor-reactive TCR_{TAG} CD8$^+$ TILs isolated from liver cancer, were analyzed from the RNAseq dataset GSE89307 (Schietinger et al., 2016). The heatmap shows the mRNA expression normalized in row Z-score.

(B) Validation of anti-CD36 antibody clone CRF D-2712 for surface staining in murine samples. The expression of CD36 and PD-1 was measured by flow cytometry in *Cd36*$^{+/+}$ or *Cd36*$^{-/-}$ CD8$^+$ TILs from MC38 tumors. Anti-CD36 antibodies clone CRF D2712 and clone HM36 were tested.

(C) The expression of CD36 and PD-1 was measured by flow cytometry in LCMV Armstrong effector CD8$^+$ T cells (15 dpi) isolated from liver or liver TCR_{TAG} CD8$^+$ TILs (15 days post tumor initiation).

(D) The expression of CD36 and FOXP3 was measured by flow cytometry in splenic CD4$^+$ T cells (CD4$^+$ sp) and CD4$^+$ TILs from B16 tumors or MC38 tumors.

(E) The expression of CD36 and PD-1 was measured by flow cytometry in CD8$^+$ TILs from B16 tumors 12 days post implantation.

(F) The expression of CD36 was measured by flow cytometry in CD8$^+$ TILs from B16 tumors 10-12 days (early) vs. 20-24 days (late) post implantation.

(G) The expression of TIM-3, TOX, TNF, IFNγ, and GZMB were measured in CD44$^+$ CD8$^+$ TILs from B16 tumors.

(H) The expression of TNF, IFNγ, or GZMB was measured in an effector cell subset ($CD44^+$ $PD\text{-}1^-$ $TIM\text{-}3^-$), an intermediate exhausted subset ($CD44^+$ $PD\text{-}1^+$ $TIM\text{-}3^-$), and a terminally exhausted subset ($CD44^+$ $PD\text{-}1^+$ $TIM\text{-}3^+$) of $CD8^+$ TILs from B16 tumors.

(I) The gating strategy for subsetting $CD8^+$ TILs from B16 tumors for Figure 2D.

(J) Human PBMCs were transduced with either empty lentivirus (EV), or lentivirus expressing CD36 (CD36 OE), and cryopreserved 72 hrs post transduction. The expression of CD36, CD4 and CD8 was measured by flow cytometry in the cells 72 hrs post transduction (Fresh) or in the cells recovered from cryopreservation (Frozen-thawed).

Data shown are mean ± SEM. Statistical analyses for (C, D, F, and H) were performed by two-tailed unpaired Student's t-test, *$p < 0.05$, **$p < 0.01$, ***$p < 0.001$. Samples were pooled from 2-3 experiments with each group containing n=6 (C), 6-9 (D), 6 (F), 9-18 (H) animals.

Figure S3. CD36 promotes $CD8^+$ TIL dysfunction

(A-L) C57BL/6J mice were implanted with B16 or MC38 tumor cells as indicated below and tumors or splenocytes were examined 21 days later.

(A-C) The expression of IFNγ was measured in $Cd36^{+/+}$ or $Cd36^{-/-}$ $CD8^+$ TILs from B16 tumors (A) and MC38 tumors (B), P14 $Cd36^{+/+}$ or $Cd36^{-/-}$ from B16 tumors (C).

(D-E) The expression of PD-1 and TIM-3 was measured in $Cd36^{+/+}$ or $Cd36^{-/-}$ $CD8^+$ TILs from B16 (D) or MC38 tumors (E) via flow cytometry. The percentage of PD-1 or TIM-3 -expressing $CD8^+$ TILs was shown.

(F-G) The gating strategy for $CD4^+$ TILs from B16 tumors (F), and the expression of FOXP3 was measured in total $CD4^+$ TILs, or the expression of TNF and IFNγ was measured in $FOXP3^-$ $CD4^+$ TILs ($CD4^+$ Tconv) (G).

(H-K) scRNAseq was performed in $Cd36^{+/+}$ or $Cd36^{-/-}$ TILs from B16 tumors. (H) UMAP plot of $Cd36^{+/+}$ or $Cd36^{-/-}$ $CD8^+$ TILs. (I) Violin plot of top 1~2 expressed genes in individual clusters ($Cd36^{+/+}$ and $Cd36^{-/-}$ TILs combined). (J) Fraction of individual clusters in $Cd36^{+/+}$ or $Cd36^{-/-}$ $CD8^+$ TILs. (K) Violin plot + boxplot of differentially expressed genes. The analyses in individual plots were restricted to cells whose expression of a given gene was great than 0.

(L) The expression of PD-1 and TIM-3 was measured via flow cytometry in $CD8^+$ TILs from B16 tumors treated with either IgA or αCD36 blockade. The percentage of PD-1 or TIM-3 -expressing $CD8^+$ TILs was shown.

Data shown are mean ± SEM. Statistical analyses for (A-E, G, and L) were performed by two-tailed unpaired Student's t-test, NS, none-significant, *$p < 0.05$, **$p < 0.01$. Samples were pooled from 2-4 experiments with each group containing n=10-13 (A), 10-13 (B), 12-13 (C), 19-29 (D), 4-12 (E), 9-19 (G), 4-5 (L) animals.

Figure S4. The impact of CD36 on metabolic activities of $CD8^+$ TILs

(A-G) *Cd36*$^{+/+}$ or *Cd36*$^{-/-}$ mice were implanted with B16 tumor cells and tumors were examined 21 days later.

(A-F) Uptake of Bodipy C12 (A), Bodipy C16 (B), uptake of cholesterol (C), neutral lipid content (D), mitochondrial potential (MitoTracker™ Deep Red FM) (E) and fatty acid oxidation (F) were measured in *Cd36*$^{+/+}$ and *Cd36*$^{-/-}$ CD8^{+} TILs.

(G) The expression of CD3, CD8, PD-1, CD36, and OxLDL uptake in *Cd36*$^{-/-}$ CD8^{+} TILs were measured by Amnis ImageStream flow cytometry. The colocalization of CD36 and OxLDL was quantified in the total *Cd36*$^{+/+}$ CD8^{+} TILs based on the Bright Detail Similarity score computed by the Amnis.

Data shown are mean ± SEM. Statistical analyses for (A-F) were performed by two-tailed unpaired Student's t-test, NS, none-significant. Samples were pooled from 2-3 experiments with each group containing n=4-7 (A), 5-7 (B-C), 4-6 (D), 6 (E), and 5-6 (F) animals.

Figure S5. The impact of OxLDL on viability, cytokine production and proliferation of CD8^{+} T cells *in vitro*

(A) Human PBMCs were activated by CD3/CD28/CD2 T Cell Activator in the presence of either vehicle control (Ctrl), OxLDL (50 μg/ml), LDL (50 μg/ml) or HDL (50 μg/ml), SSO (100 μM), or SSO + OxLDL for 6 days. Viability was assessed via Live Dead assay by flow cytometry.

(B) Human PBMCs were activated by CD3/CD28/CD2 T Cell Activator in the presence of either vehicle control (Ctrl), or different concentrations of OxLDL for 6 days. TNF and IFNγ were then measured upon re-stimulation with PMA/Ionomycin for 4 hours and analyzed by flow cytometry.

(C) P14 splenic CD8^{+} T cells were *in vitro* activated for 48 hrs, and then treated with vehicle control (Ctrl), OxLDL (50 μg/ml), LDL (50 μg/ml) or HDL (50 μg/ml), SSO (100 μM), or SSO + OxLDL for another 24 hrs. Viability was assessed via Live Dead assay by flow cytometry.

(D) P14 or OT-1 splenic CD8^{+} T cells were *in vitro* activated for 48 hrs, and then treated with vehicle control (Ctrl), or different concentrations of OxLDL for another 16~24 hrs. TNF, IFNγ, GZMB, or cell viability were then measured upon re-stimulation with cognate peptide for 6 hours and analyzed by flow cytometry.

(E) Naïve P14 splenocytes were labeled with CFSE, and *in vitro* activated for 48 hrs. Cells were then treated with vehicle control (Ctrl), LDL (50 μg/ml) or OxLDL (25 or 50 μg/ml) for another 24 hrs. CFSE intensity in live CD8^{+} T cells was measured via flow cytometry.

Data shown are mean ± SEM. Statistical analyses for (B and D) were performed by two-tailed unpaired one-sample Student's t-test against control, * $p < 0.05$, ** $p < 0.01$, *** $p < 0.001$. Samples were representative from 2 experiments (B), or pooled from 3 experiments with each group containing n=6-9 (D).

Figure S6. OxLDL induces CD36 expression in CD8 T cells in vitro

P14 or OT-1 splenocytes were *in vitro* activated for 48 hrs, and then treated with vehicle control (Ctrl), or different concentrations of OxLDL for another 24 hrs. CD36 expression was analyzed by flow cytometry.

Data shown are mean ± SEM. Statistical analyses were performed by two-tailed unpaired Student's t-test, * $p < 0.05$, ** $p < 0.01$, *** $p < 0.001$. Samples were pooled from 2-3 experiments with each group containing n=4-7.

Figure S7. GPX4 OE restores $CD8^+$ T cell function in tumors

P14 naïve $CD8^+$ T cells were *in vitro* activated for 24 hrs, and then transduced with either empty retrovirus (EV) or a retrovirus overexpressing *Gpx4* (GPX4 OE). Congenically distinct 5×10^5 EV cells and 5×10^5 GPX4 OE cells were mixed at a ratio of 1:1, and transferred into C57BL/6J mice implanted with B16-gp33 tumors. EV and GPX4 OE $P14^+$ donor TILs were analyzed at 10 days post transfer by flow cytometry for IFNγ and TNF cytokine production.

Statistical analyses were performed by two-tailed paired Student's t-test, NS, none-significant, ** $p < 0.01$. Each group containing n=5.